Outskirts of Galaxy Clusters: Intense Life in the Suburbs
Proceedings IAU Colloquium No. 195, 2004
A. Diaferio, ed.

DOI: 10.1017/S1743921304000808

Wide field imaging of distant clusters

Tommaso Treu

Division of Astronomy & Astrophysics University of California, Los Angeles, CA 90095-1562, USA email: ttreu@astro.ucla.edu

Abstract. Wide field imaging is key to understanding the build-up of distant clusters and their galaxy population. By focusing on the so far unexplored outskirts of clusters, where infalling galaxies first hit the cluster potential and the hot intracluster medium, we can help separate cosmological field galaxy evolution from that driven by environment. I present a selection of recent advancements in this area, with particular emphasis on Hubble Space Telescope wide field imaging, for its superior capability to deliver galaxy morphologies and precise shear maps of distant clusters.

1. Introduction

In the current standard cosmological paradigm (see, e.g., talks by Benson, Moore, Springel, Tormen), clusters of galaxies form in correspondence with the first overdensities in the early universe and grow by mergers and by accreting material from the surrounding regions (which I will generally refer to as the *field*).

In this scenario, the infall regions of clusters are believed to be very important – as testified by the enthusiastic participants of this meeting. As galaxies, gas, and dark matter are accreted onto the cluster, they are subject to interactions with the steep gravitational potential, along with the galaxies and hot plasma already present in the cluster. Under appropriate conditions, the outcome of these interactions can be quite dramatic, e.g., altering the morphology and star formation properties of infalling galaxies (e.g. Mastropietro's talk).

In this contribution I will focus on two particular aspects of the physics of the infall regions: i) the environmental effects on the morphological properties of galaxies and ii) the distribution of dark matter. As suggested by Antonaldo and the Scientific Organizing Committee, I will focus on wide field (> 1 Mpc radius) imaging of distant clusters as a diagnostic tool to study these processes (for other diagnostic tools see talks by, e.g., Balogh, Dressler, Ellingson, Moran, Poggianti). Studying distant clusters ($z > 0.1$) provides two important pieces of information. One the one hand, distant clusters are efficient gravitational lenses and therefore weak and strong lensing can be used to characterize their mass distribution (see also Schneider's talk). On the other hand, with current technology it is possible to reach look-back times of several Gyrs, i.e comparable to the evolutionary time-scales for these systems. Therefore, by comparing local clusters to their "progenitors"†, we can aim at empirically mapping the cosmic evolution of the infall regions. Due to space limitations, I will restrict my contribution to a personal selection of observational results. Most of them are obtained with the *Hubble Space Telescope*, for its ability to determine galaxy morphology and measure lensing signals.

The Hubble constant, the matter density, and the cosmological constant are assumed to be $\mathrm{H}_0 = 65\ \mathrm{km\,s^{-1}\,Mpc^{-1}}$, $\Omega_\mathrm{m} = 0.3$, and $\Omega_\Lambda = 0.7$, throughout this paper.

† With all due cautionary notes on this crucial step.

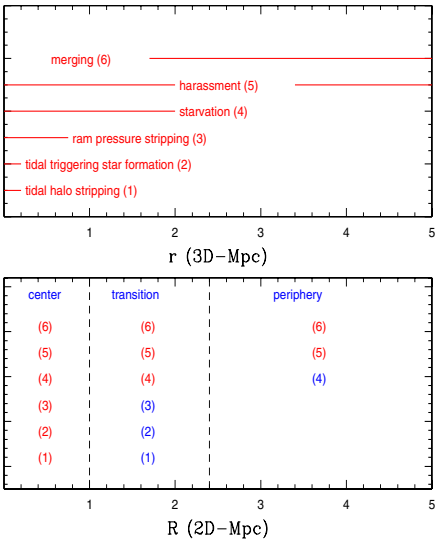

Figure 1. Summary of spheres of influence for key physical mechanisms in the galaxy cluster CL0024 ($z = 0.39$). Top panel: the horizontal lines indicate the radial region where the mechanisms are most effective (in 3-D space; note that the harassment is effective in the entire range). Lower panel: for each projected annulus we identify the mechanisms that can have affected the galaxy in the region (red). The blue numbers indicate processes that are marginally at work. See T03 for additional discussion (reproduced with permission).

2. Environmental processes and physical scales

It is empirically known that the mix of morphological types is a function of local galaxy density (Dressler 1980) and redshift (Dressler et al. 1997; Treu et al. 2003, hereafter T03; Smith et al. 2004). This is generally interpreted as the combination of two mechanisms. Firstly, high density regions are very special places in the Universe and therefore galaxies observed there might have formed under special initial conditions. Secondly, interactions between galaxies, dark matter and the intra–cluster medium (i.e. environmental processes) are likely to transform in–falling field galaxies from gas–rich spirals to gas–poor lenticular galaxies. In some sense, understanding the balance between the two processes can be thought of as a nature vs. nurture problem, although certainly the distinction is somewhat arbitrary (the environment a galaxy is formed in is, in a broad sense, part of the initial conditions). Therefore, I will use the following simplified formulation of the problem. Let us consider a general population of *field* galaxies and let them fall into a cluster. When (and if) they arrive at the cluster center, will they have changed their distribution of morphologies, as a result of interactions, so as to match that of high density regions? If the answer is no, then we have to invoke different initial conditions (e.g. mass function). If the answer is yes, then we would like to know exactly which physical mechanism is doing what.

Assuming the answer to the former question is "yes" or "in part", in order to address the latter issue (what physical mechanism is doing what) it is useful to rank the proposed mechanisms by estimating the relevant time and length scales. In the upper panel of Figure 1, I show spheres of influence for various physical mechanisms (computed as an example for CL0024 at $z = 0.39$, see T03 for definitions and details). The lower panel shows two–dimensional spheres of influence once projection effects, duration of phenomena, and travel times are taken into account (see discussion of the "back-splash"-

https://doi.org/10.1017/S1743921304000808 Published online by Cambridge University Press

effect in Ellingson's and Moore's talks). It is clear that the center of the cluster is a very busy environment, where many processes are simultaneously at work. By contrast, the outer regions – the *transition* region around the virial radius and the *periphery* beyond that – provide a much cleaner environment, and therefore the opportunity to separate the effects of different mechanisms.

3. Wide field imaging

3.1. *Ground based studies*

One of the key difficulties in interpreting wide field imaging data in terms of galaxy population is identifying cluster members at large radii, where the contrast over the background/foreground is low. Abraham et al. (1996) made an important step forward in this respect by obtaining unprecedented spectroscopic follow-up – including hundreds of members – of the $z = 0.228$ cluster A2390. They obtained the first observational constraints on the infall scenario, finding that the properties of galaxies – such as colors and spectral features – changed smoothly with radius, consistent with an idea of gradual infall without significant mixing (see also Morris et al. 1998). The recent development of wide field imagers and spectrographs on big telescopes – with the ability to obtain hundreds of redshift at a time – seems to suggest that we will see more studies of this kind in the next years, with even larger redshift catalogs (Czoske at this meeting presented an ongoing project collecting *thousands* of redshifts per cluster).

To tackle the same problem, Kodama et al. (2001) followed a different approach. They used photometric redshifts based on high quality Subaru images to identify galaxies in a relatively thin redshift slice around the cluster A851 ($z = 0.39$). Although some residual contamination is present, the use of photometric redshifts allowed them to study an even larger sample of galaxies to fainter intrinsic luminosities. Based on this technique, they were able to convincingly show the filamentary structure of the accreting material. They also detected a rapid transition in galaxy colors at a characteristic density, possibly the signature of environmental processes influencing infalling galaxies (see also Gray's talk).

3.2. *HST-WFPC2 studies*

The Wide Field and Planetary Camera 2 (WFPC2) revolutionized the subject, by delivering images of galaxies in† distant clusters with sufficient resolution to accurately measure their shapes and morphologies (e.g. Couch et al. 1994; Dressler et al. 1994; Ellis et al. 1997). Unfortunately, the 4 800x800 pixel^2 CCDs provide a field of view of only ~ 2.5 arcmin on a side, corresponding to less than a Mpc at $z \sim 0.5$. Hence, performing wide field studies of distant clusters requires patient and expensive mosaicing. Using contiguous pointings, Couch et al. (1998) and van Dokkum et al. (1998) constructed the morphology-density relation and color-magnitude relation reaching the *transition* region of two clusters at $z \sim 0.3$. They found that the morphology density relations starts to flatten out beyond $\sim$ 1Mpc and that the color-magnitude relation of lenticular galaxies is less tight than in the cluster core (but see Andreon 1998 for an explanation of this latter finding in terms of morphological classification uncertainties). WFPC2 mosaics of comparable size have been obtained now for a few clusters (e.g. talks by Dressler and Tran).

In order to reach significantly beyond 1 Mpc in a finite number of HST orbits, T03 adopted a sparse sampling strategy. With 39 WFPC2 pointings they covered a circle 10 Mpc in diameter, with fractional area coverage 20-40% in the *transition* and *periphery*

† Or behind, for weak lensing purposes.

https://doi.org/10.1017/S1743921304000808 Published online by Cambridge University Press

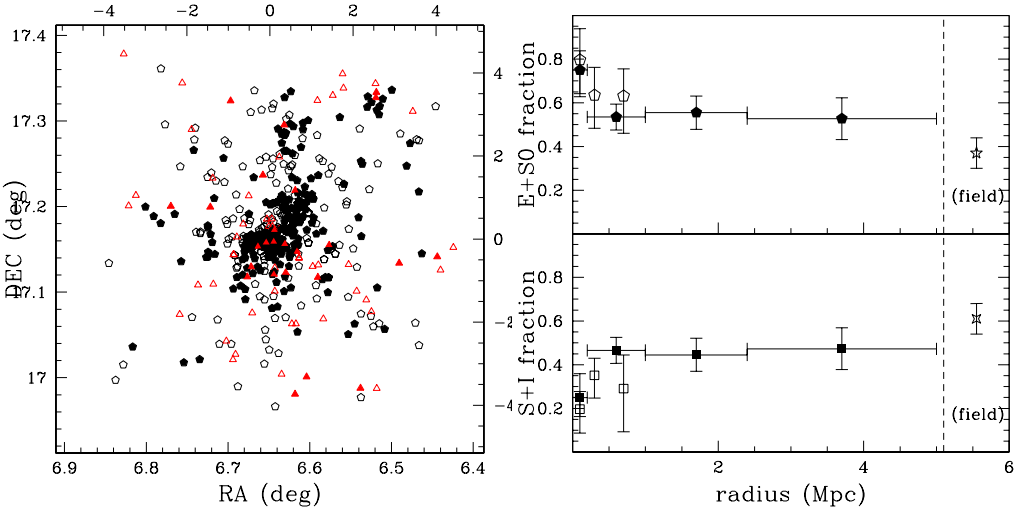

Figure 2. Left: Projected distribution of CL0024 member galaxies. Solid symbols indicate objects with available HST-WFPC2 images. The top and right scale is in Mpc. Right: Fraction of morphological types ($I < 21.1$) in CL0024+16 as a function of cluster radius: (upper panel) fraction of E+S0 galaxies; (lower panels) fraction of spirals. Fractions determined from the entire WFPC2 sample – removing the background statistically – are shown as large empty points, while fractions determined from the spectroscopic WFPC2-z catalog are shown as solid points. Points beyond the dashed line at 5.1 Mpc are field fractions. From T03 (reproduced with permission).

regions of cluster CL0024 at $z \sim 0.39$. More than 1300 redshifts, including those of 472 members, are available to identify cluster members at the periphery of the cluster.

The left panel of Figure 2 shows an updated map of the cluster (superceding that in T03) members. By combining HST data and redshift, the morphology-radius relation can be measured for a single system out to almost 5 Mpc (Figure 2, right panel; from T03, updated to include the complete redshift catalog). Beyond 1 Mpc the fraction of early-type galaxies declines gently with radius toward the lower field value. This gradient cannot be caused by mechanisms such as ram-pressure stripping or tidal interaction with the main cluster potential.

The distribution of galaxies is clearly not circularly symmetric, as show in the left panels of Figures 2 and 3. Therefore, we can learn more about the relationship between morphology and environmental effects by studying the morphology-density relation as a function of location inside the cluster (right panel of Figure 3). Remarkably, the morphology density relation does not depend – within the uncertainties – on the location inside the cluster. At a given density, the morphological mix appears to be independent of the cluster radius. A direct implication of this finding is that galaxy concentrations outside the central peak are physically associated and therefore galaxies are not accreted as individuals but rather as groups, with their own hierarchy of morphologies (and dark matter halos as I discuss later). At least part of the morphological transformations could happen at the group level where galaxies are "pre-processed" before entering the cluster. At the group level, different physical mechanisms are at work (e.g. merging is more frequent, ram pressure stripping is less effective), and therefore it is possible that different mechanisms dominate at subsequent stages.

The sparse sampled mosaic of CL0024 can also be used to study the dark matter distribution in the infall regions. A joint weak and strong lensing analysis (Kneib et

https://doi.org/10.1017/S1743921304000808 Published online by Cambridge University Press

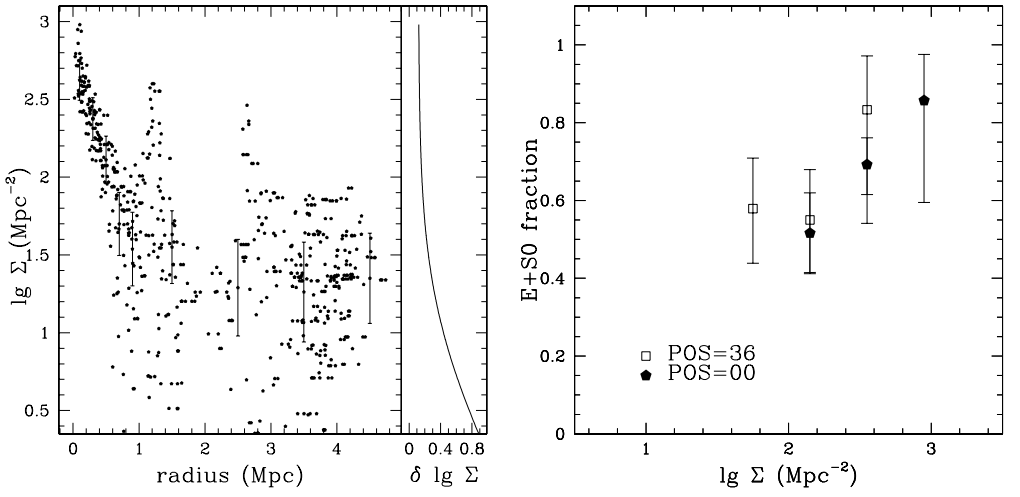

Figure 3. Left: Local surface density vs cluster radius in CL0024 revealing the large range at a given radius and the spike in local density at ~ 1 Mpc. The points with error bars indicate the average Σ within radial bins, and the scatter expected from measurement errors. The expected uncertainty as a function of Σ is shown in the right panel. Right: Fraction of E+S0 galaxies in CL0024+16 as a function of local projected density for galaxies in the central (solid pentagons) and in the NW overdensity region (open squares; POS36) corresponding to the spike in local density at ~ 1 Mpc in the left panel. Note the close match in the regions of overlapping density. From T03 (reproduced with permission).

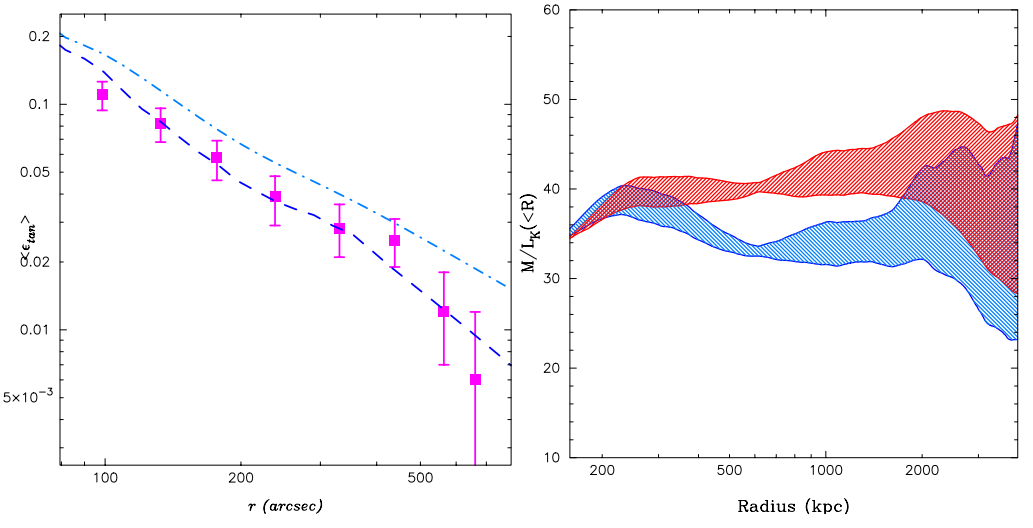

Figure 4. Left: Reduced tangential shear profile of CL0024 for the combined WFPC2 and STIS data (magenta points with error bars). The dashed line is the visual representation of the reduced tangential shear of the 2 clump NFW model that best fits both the strong and weak lensing constraints. The dot-dashed line corresponds to the reduced tangential shear of the 2 clump SIS model that best fits the strong lensing constraints but fails to fit the weak lensing measurements. Right: M/L_K ratio (rest frame solar units) of CL0024 . The (blue) lower hatched region corresponds to the M/L derived for the enclosed field-subtracted K-band sample and the (red) upper hatched region that for the color-selected sample. From K03 (reproduced with permission).

https://doi.org/10.1017/S1743921304000808 Published online by Cambridge University Press

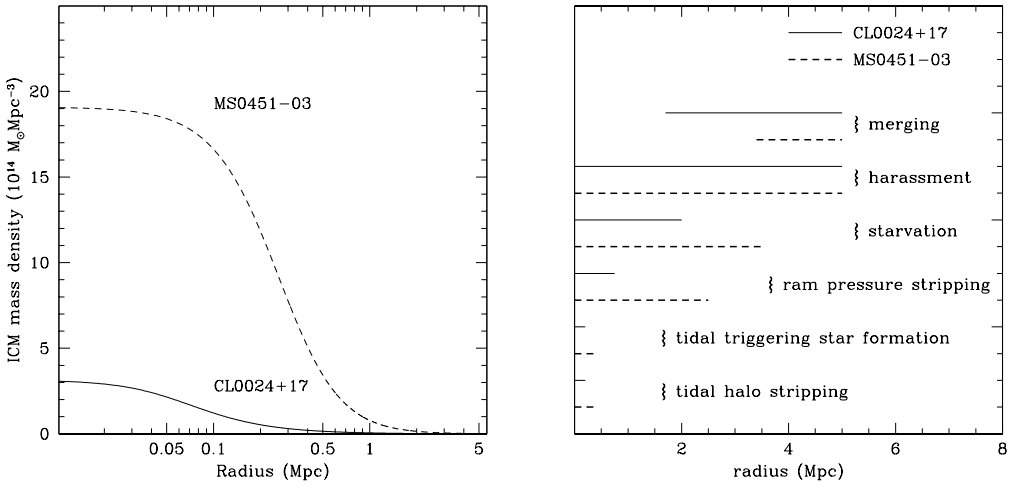

Figure 5. Left: comparison of the mass density profile of the intracluster medium (ICM) in CL0024+17 and MS0451-03. Right: Comparison of the regions of influence of key physical mechanisms for CL0024+17 and MS0451-03. Note the dramatic enhancement in the size of the sphere of influence of the ICM – ram pressure stripping and starvation – in MS0451-03.

al. 2003; hereafter K03) reveals the presence of a secondary clump of mass, coincident with the overdensity of galaxies 1 Mpc NW of the cluster core identified in Figures 2 and 3, with mass-to-light ratio consistent with that of the main clump. After appropriate azimuthal averaging, the lensing analysis can be extended to the periphery, resulting in the mass shear profile shown in the left panel of Figure 4. The joint weak and strong lensing constraints are consistent with a Navarro, Frenk & White (1997) mass profile outside the central region, and inconsistent with a singular isothermal sphere (c.f. talks by Biviano and Mamon). The right panel of Figure 4 shows the rest frame K-band mass-to-light ratio of the cluster, which is approximately constant all the way out to the periphery, indicating that the infalling material has approximately the same fraction of mass in stars as the central regions. A similar result for local clusters – based on a completely independent "caustic" technique (Diaferio & Geller 1997; Diaferio 1999) – was shown as this meeting by Rines. Remarkably, the M/L_K of CL0024 is consistent with that of local clusters, once a correction corresponding to passive evolution of an old stellar population is applied.

3.3. *HST-ACS studies*

The successful installation of the Advanced Camera for Surveys (ACS) on board HST has improved its ability to carry out wide field imaging of distant clusters by a factor of 10 (considering area and depth). Several wide field studies are currently ongoing, including for example the ACS GTO cluster program, and the follow-up of MS1054 ($z = 0.83$) by Kelson et al. This improvement makes it possible to obtain fully sampled mosaic of distant clusters over diameters corresponding to several virial radii. It is of particular interest to study and contrast the properties of galaxies in clusters with different intracluster medium (ICM) properties. For example, MS0451 ($z = 0.54$; covered by GO-9836, PI Ellis) is a rich cluster, much more luminous in the X-ray than CL0024. Figure 5 illustrates the different ICM content of the two clusters and compares the spheres of influences of the various processes in the two clusters. ICM related mechanisms, such as ram-pressure stripping and starvation, have larger spheres of influence in MS0451 than in CL0024.

https://doi.org/10.1017/S1743921304000808 Published online by Cambridge University Press

With so many exciting projects on their way, and the warm hospitality of Torino, I hope that the organizing committee will reconvene another meeting on the subject in the near future.

Acknowledgements

It is a pleasure to acknowledge the numerous and valuable contributions of my collaborators – Oliver Czoske, Alan Dressler, Patrick Hudelot, Jean-Paul Kneib, Phil Marshall, Sean Moran, Priya Natarajan, Gus Oemler, Graham Smith, Ian Smail – to the work presented here. I am especially grateful to Richard Ellis for his invaluable scientific contributions and much appreciated advice and support. Finally, I would like to thank the organizers of this meeting for the exciting scientific program, and for inviting me. Financial support from IAU and from NASA through Hubble Fellowship grant HF-01167.01 is gratefully acknowledged.

References

Abraham, R. et al. 1996 *ApJ* **471**, 694–719.
Andreon, S. 1998 *ApJ* **501**, 533–538.
Couch, W.J., Barger, A. J., Smail, I., Ellis, R. S., Sharples, R. M. 1994 *ApJ* **430**, 121–138.
Diaferio, A. 1999, *MNRAS* **309**, 610–622.
Diaferio, A. & Geller, M. J. 1997, *ApJ* **481**, 633–643.
Dressler, A. 1980 *ApJ* **236**, 351–365.
Dressler, A., Oemler, A. Jr., Butcher, H. R., Gunn, J. E. 1994 *ApJ* **435**, L23–L26.
Dressler, A. et al. 1997 *ApJ* **490**, 577–591.
Ellis, R. S., Smail, I., Dressler, A., Couch, W. J., Oemler, A. Jr., Butcher, H., Sharples, R. M. 1997 *ApJ* **483**, 582–596.
Kneib, J.-P.. et al. 2003 *ApJ* **598**, 804–817.
Kodama, T., Smail, I., Nakata, F., Okamura, S., Bower, R. G. 2001 *ApJ* **562**, L9–L12
Morris, S. L., Hutchings, J. B., Carlberg, R. G., Yee, H. K. C., Ellingson, E., Balogh, M. L., Abraham, R. G., Smecker-Hane, T. A. 1998 *ApJ* **507**, 84–101.
Navarro, J., Frenk, C. & White S. 1997 *ApJ* **490**, 493–508.
Smith, G.P., Treu, T., Ellis, R.S. Moran, S.M., Dressler A. 2004 *ApJ, submitted, astro-ph/0403455*
Treu, T., Ellis, R. S., Kneib, J.-P., Dressler, A., Smail, I., Czoske, O., Oemler, A., Natarajan, P. 2003 *ApJ* **591**, 53–78.
van Dokkum, P. G., Franx, M., Kelson, D. D., Illingworth, G. D., Fisher, D., Fabricant, D. 1998 *ApJ* **500**, 714–737.